ACS Partner Journal

CHEMICAL & BIOMEDICAL IMAGING

pubs.acs.org/ChemBioImaging

Article

Synthesis and Characterization of a Novel Photocleavable Fluorescent Dye Dyad for Diffusion Imaging

Damian Schöngen and Dominik Wöll*

Cite This: *Chem. Biomed. Imaging* 2025, 3, 199−207

Read Online

ACCESS | Metrics & More | Article Recommendations | Supporting Information

ABSTRACT: We report the synthesis and characterization of a photocleavable fluorescent dye dyad. The two constituting dyes show a large spectral overlap and are in close proximity to each other, leading to efficient Förster Resonance Energy Transfer (FRET). Photocleavage of the dyad and the subsequent independent diffusion of both fluorophores qualifies the system to be used for high accuracy diffusion measurements. In contrast to previous work, the dyad reported here can be applied in polar solvents and cleaved by UV-A light. Beneficially, the photolabile linker provides two orthogonal labeling sites for various commercially available fluorescent labels. In this work, we chose the cationic organic dyes ATTO565 and ATTO647N. We outline the synthesis and spectral characterization of the system with UV−Vis and fluorescence spectroscopy as well as fluorescence lifetime and fluorescence quantum yield measurements. Furthermore, we performed proof-of-principle microscopy experiments to demonstrate its capability in polyvinyl acetate films.

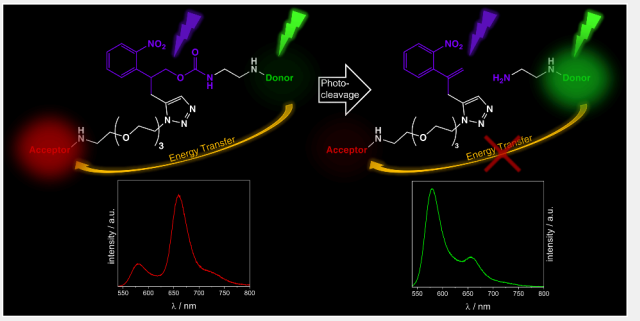

KEYWORDS:
single molecule FRET; diffusion measurements; single molecule fluorescence microscopy; photocleavable compounds; polymer dynamics

INTRODUCTION

Diffusion processes are fundamental to a wide range of scientific disciplines and applications. The mass transport in biological cells, catalysis and most reactions in general are governed by diffusion.[2,3] Likewise, the understanding of membrane dynamics, e.g. in fuel cells and separation applications, is dependent on accurate diffusion measurements.[4−6] Numerous studies have been published on the subject matter of diffusion in biological systems.[7−15] In addition, there has been a notable increase in interest in the diffusion processes of nonbiological polymeric systems in recent years.[4,16−22] Several powerful techniques such as Pulsed Field Gradient Nuclear Magnetic Resonance (PFG NMR),[23,24] Fluorescence Recovery After Photobleaching (FRAP)[12,25,26] or Fluorescence Correlation Spectroscopy (FCS)[27,28] have been developed. Yet, as ensemble techniques, they cannot reveal diffusional or structural inhomogeneities.[15,19,20] Methods like Single Particle or Single Molecule Tracking (SPT and SMT) circumvent averaging and gave totally new insights into the heterogeneity of various systems.[29,30] In cases of very slow diffusion, however, these methods suffer from limitations, as the accuracy is, among other things, dependent on the number of collected photons[31] and the mechanical stability of the measurement setup.[1] Taking into account localization inaccuracies caused by low signal-to-noise-ratio due to low signal or non-negligible background[32] and dye orientation,[33] diffusion coefficients below $D \approx 10^{-17}$ m^2 s^{-1} can no longer be measured reasonably with either SPT or SMT. New sophisticated single molecule approaches like minimal fluorescence photon fluxes microscopy (MINFLUX) surpass even this limit.[34] However, elaborate equipment is required and MINFLUX is restricted to confocal microscopy.

We developed a novel single molecule method for highly accurate measurements of low diffusion coefficients.[1] In the present work, we named this method FRET Efficiency Diffusion measurement Upon Photocleavage (FEDUP). For FEDUP, a FRET donorFRET acceptor dyad is used with the fluorophors connected via a photocleavage group.[35] Thus, initially the energy transfer process is very efficient. It should be noted that it has been shown that a simple FRET (dipole−dipole) mechanism is a simplification for two dyes in close proximity and that real systems show significant deviation from this model.[36] However, for our analysis it is of primary importance that distances smaller than the Förster radius show high energy transfer efficiency whereas the FRET efficiency

Received: October 31, 2024
Revised: February 7, 2025
Accepted: February 10, 2025
Published: February 21, 2025

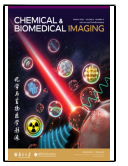

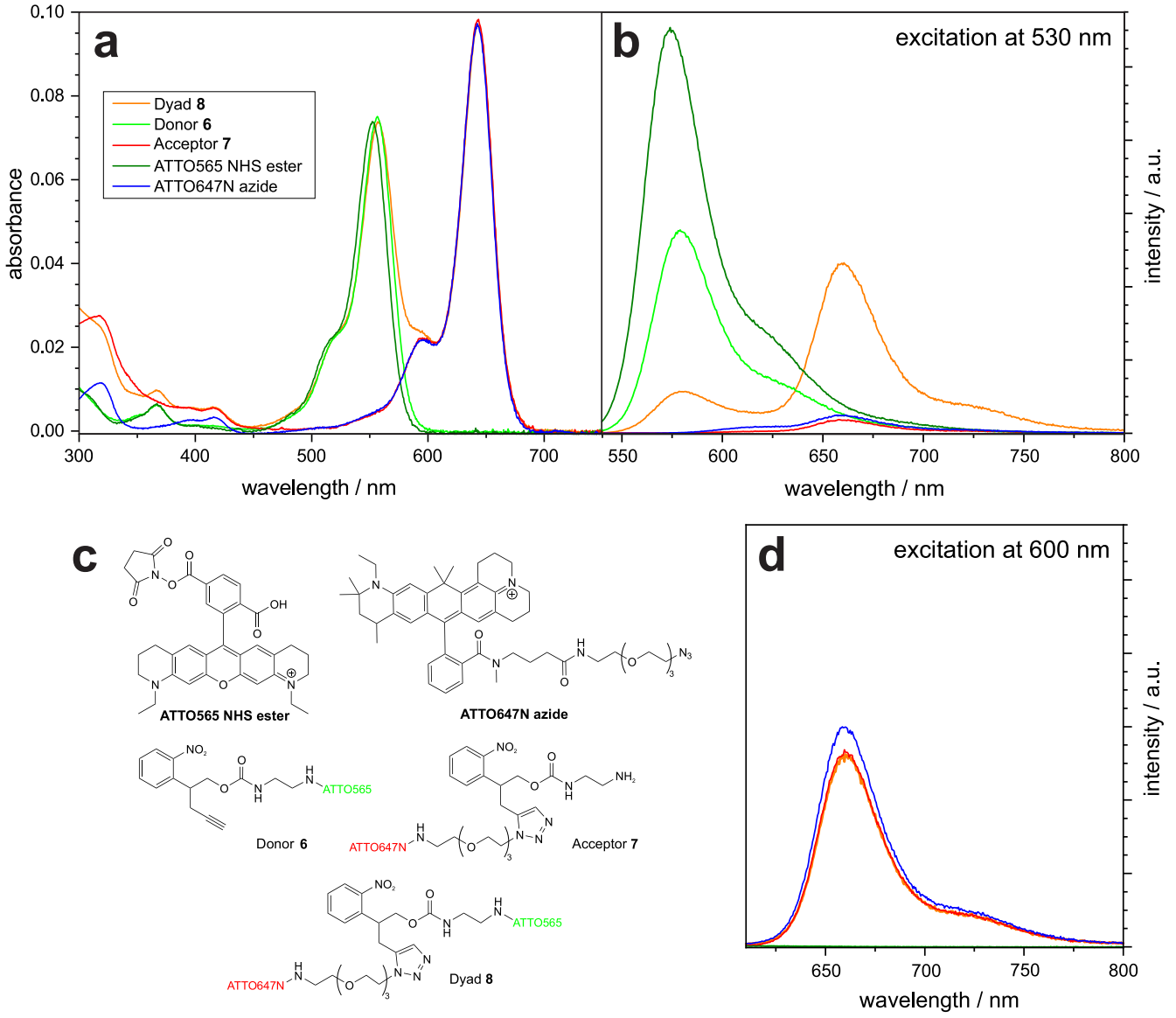

Figure 1. (a) Absorption and (b) emission (excitation at 530 nm) spectra of **ATTO565 NHS ester** (olive), **ATTO647N azide** (blue), reference donor **6** (green), reference acceptor **7** (red), and dyad **8** (orange) in methanol. All compounds are shown in (c). The corresponding emission spectra with 600 nm excitation are presented in (d). No significant excitation was observed for the compounds without ATTO647N moiety. The concentration of all compounds was adjusted to approximately 0.6 μmolL^{-1}.

decreases with increasing distance with the well-known distance dependence to the power of six. The point of photocleavage determines the time at which the two fluorophores begin to diffuse independently. The resulting time trace, together with the Förster radius, allows for the calculation of a diffusion coefficient. The method can be integrated into both widefield and confocal set-ups with comparatively little effort, as long as sufficient spectral resolution is ensured. FEDUP is largely independent of localization precision and its inherent limitations, since accurate spatiotemporal information is obtained from either intensities or lifetimes of single emitters. So far, we have reported one photocleavable FRET dyad that has been limited to diffusion measurements in hydrophobic environments due to the choice of dyes.[1] Furthermore, the former molecule requires UV light with wavelengths smaller than 320 nm and, thus, limits the transmission through the typical optics used in optical microscopy. Here, we report the synthesis and photochemical characterization of a novel photocleavable fluorescent dye dyad with enhanced hydrophilicity and the possibility to be cleaved with more suitable UV wavelengths up to 400 nm. Microscopy experiments demonstrate that the dyad can be applied to highly accurate diffusion measurements in polar systems. Thus, the improved properties of the novel dyad allows for its application in both life science and material science systems.

RESULTS AND DISCUSSION

Spectroscopic Characterization of the Dye Systems

We developed a novel FRET dyad **8** with two water-soluble dyes, ATTO565 and ATTO647N, which are an efficient FRET pair and which exhibit very high photostability. As linker between both dyes the photocleavable 2-(2-nitrophenyl)-propoxycarbonate (NPPOC) moiety was chosen due to its high photocleavage efficiency and good performance in

https://doi.org/10.1021/cbmi.4c00084
Chem. Biomed. Imaging 2025, 3, 199−207

Table 1. Fluorescence Lifetimes τ of Compounds ATTO565 NHS ester, ATTO647N azide, Energy Donor Reference Compound 6, Energy Acceptor Reference Compound 7, and Dyad 8 in Methanol before and after 1500 s of Irradiation with a 365 nm LED @ 450 W m^{-2} [a]

Compound	λ_{exc}/nm	λ_{em}/nm	τ_1(0 s)/ns	τ_2(0 s)/ns	τ_1(1500 s)/ns	τ_2(1500 s)/ns
ATTO565NHS ester	527	545−620	4.13 [100%]		4.07 [100%]	
Donor **6**	527	545−620	2.95 [73%]	2.19 [27%]	4.03 [75%]	1.56 [25%]
Dyad **8**	527	545−620	3.43 [69%]	1.94 [31%]	4.12 [91%]	1.68 [9%]
ATTO647N azide	635	655−715	4.30 [100%]		4.27 [100%]	
Acceptor **7**[b]	635	655−715	4.20 [100%]		4.17 [89%]	1.3 [11%]
Dyad **8**	635	655−715	3.76 [100%]		4.17 [82%]	1.04 [18%]
Dyad **8**	527	655−715	3.67 [100%]		3.93 [71%]	1.01 [29%]

[a]Lifetimes were determined either with 527 or 635 nm excitation. For **ATTO565 NHS ester** and donor **6** the emission between 545−620 nm was analyzed. For **ATTO647N azide** and acceptor **7** the emission between 655−715 nm was analyzed. For dyad **8**, both spectral windows were analysed separately. The amplitudes of the fluorescence lifetime components τ_1 and τ_2 are mentioned in square brackets after the lifetimes. The errors of the lifetime components are always in the order of magnitude of the last decimal place specified. [b]After additional 2200 s of UV irradiation at approximately tripled power density, the lifetimes increase again to τ_1(3700 s) = 4.21 ns (95%), τ_2(3700 s) = 1.7 ns (5%).

photolithographic oligonucleotide synthesis.[37−39] The syntheses of dyad **8** as well as two reference substances, the corresponding energy donor **6** and energy acceptor **7**, respectively, are given in the Supporting Information (Schemes S1−S8, see also Figures S31−S35). After purification, the small amounts of products of the fluorophore-containing substances were characterized with ESI-MS (see the Supporting Information (S.I.), Figures S42−S46), UV−Vis and fluorescence spectroscopy. Additionally, fluorescence lifetimes and quantum yields were determined. The absorption and emission spectra of all fluorescent compounds (in a concentration of about 0.6 μmol L^{-1}) in methanol as well as their structures are presented in Figure 1 a−d. Fluorescence lifetimes are listed in Table 1 (for TCSPC curves, see Figures S19−S26 in the S.I.). A tabular overview of the fluorescence quantum yields is given in the Supporting Information (Table S3 and Figures S4−S9). Furthermore, the purity of dyad **8** was confirmed with HPLC (see S.I., Figures S47 and S48).

In the visible range, the absorption spectra are dominated by the dye spectra of ATTO565 or ATTO647N, respectively. The absorption of the dyad **8** is an overlap of the corresponding absorbances of the reference donor and acceptor compound indicating no significant interaction of the dyes in the ground state. For excitation at 530 nm, which predominantly excites the ATTO565 fluorophore, the emission spectra of the ATTO565 NHS ester and the reference donor **6** resemble each other in appearance, but surprisingly not in their intensities. The emission of ATTO565 is reduced by almost half. A more quantitative comparison reveals a drop of the fluorescence quantum yield from 97% of ATTO565 to 61% of the reference donor **6**. Together with Stern−Volmer experiments in solution (see S.I., Figures S10−S17), we could attribute this behavior to an intramolecular quenching process caused by the nitrophenyl group of the photocleavable linker which is a known fluorescence quencher.[40,41] This quenching is also confirmed by the alteration in fluorescence lifetime which changes from one long lifetime component τ = 4.13 ns for ATTO565 to two shorter lifetime components, τ_1 = 2.95 ns and τ_2 = 2.19 ns, in a ratio of approximately 3:1 for donor **6**. We propose that the two lifetime components are average values corresponding to various conformations the donor **6** can adopt which exhibit different quenching efficiency due to variable distances between the quenching moiety and the dye moiety. Correspondingly, a similar relative decrease in fluorescence quantum yield is found. In contrast, intramolecular quenching of the energy acceptor ATTO647N by the nitrophenyl moiety is not very pronounced. Only a slight drop from 75% to 66% in the fluorescence quantum yield and a fluorescence lifetime decrease from 4.3 to 4.2 ns is observed when comparing ATTO647N azide with the reference acceptor **7**. This is consistent with our Stern−Volmer experiments which reveal a significantly stronger quenching of ATTO565 by nitro-arenes compared to ATTO647N (see S.I., Table S4).

The emission spectrum of the dyad **8** (see Figure 1b) for excitation of the donor is dominated by the emission of the acceptor. Thus, an efficient energy transfer from ATTO565 to ATTO647N occurs which can be suitably well described by a Förster energy transfer model. The reported Förster radius of ATTO565 and ATTO647N in aqueous solution is 6.9 nm.[42] From our spectra and quantum yields measured in methanol we calculated a Förster radius of R_0 = 6.23 nm for the reference donor **6** − reference acceptor **7** pair in methanol and R_0 = 6.61 nm for the pure precursor dyes, respectively, assuming free rotation of both dyes and a resulting κ^2 value of 2/3. Compared to the reference donor compound **6**, the fluorescence intensity of the dyad **8** is reduced by about 80% at 580 nm, and the intensity at 660 nm by far exceeds the intensity caused by the direct excitation of the ATTO647N when excited with 530 nm. Consequently, the Förster resonance energy transfer efficiency is approximately 80%. Given the large calculated Förster radius, it is not clear to us why the FRET efficiency is not more quantitative. Involuntary partial cleavage due to insufficient protection from UV-light, e.g. during the sample preparation, cannot be excluded. However, the lifetime measurements discussed in the following do not support this hypothesis, since no lifetime components of any cleavage compound are found in the nonirradiated samples prepared under comparable conditions. Instead, the lifetime measurements also indicate that a fraction of the energy donors in the dyad do not undergo energy transfer. In this context, it seems likely that the assumption of free rotation of both dyes in the dyad is invalid. The energy transfer is also a rational explanation for the observed fluorescence lifetime values of donor **6** and dyad **8** (see Table 1). In the spectral emission window of the donor between 545 and 620 nm the fluorescence decay of dyad **8** exhibits two lifetime components, τ_1 = 3.43 ns (69%) and τ_2 = 1.94 ns (31%), similar in magnitudes and amplitudes to the ones of the donor **6**. The slight divergence can be explained by the fact that the donor

https://doi.org/10.1021/cbmi.4c00084
Chem. Biomed. Imaging 2025, 3, 199−207

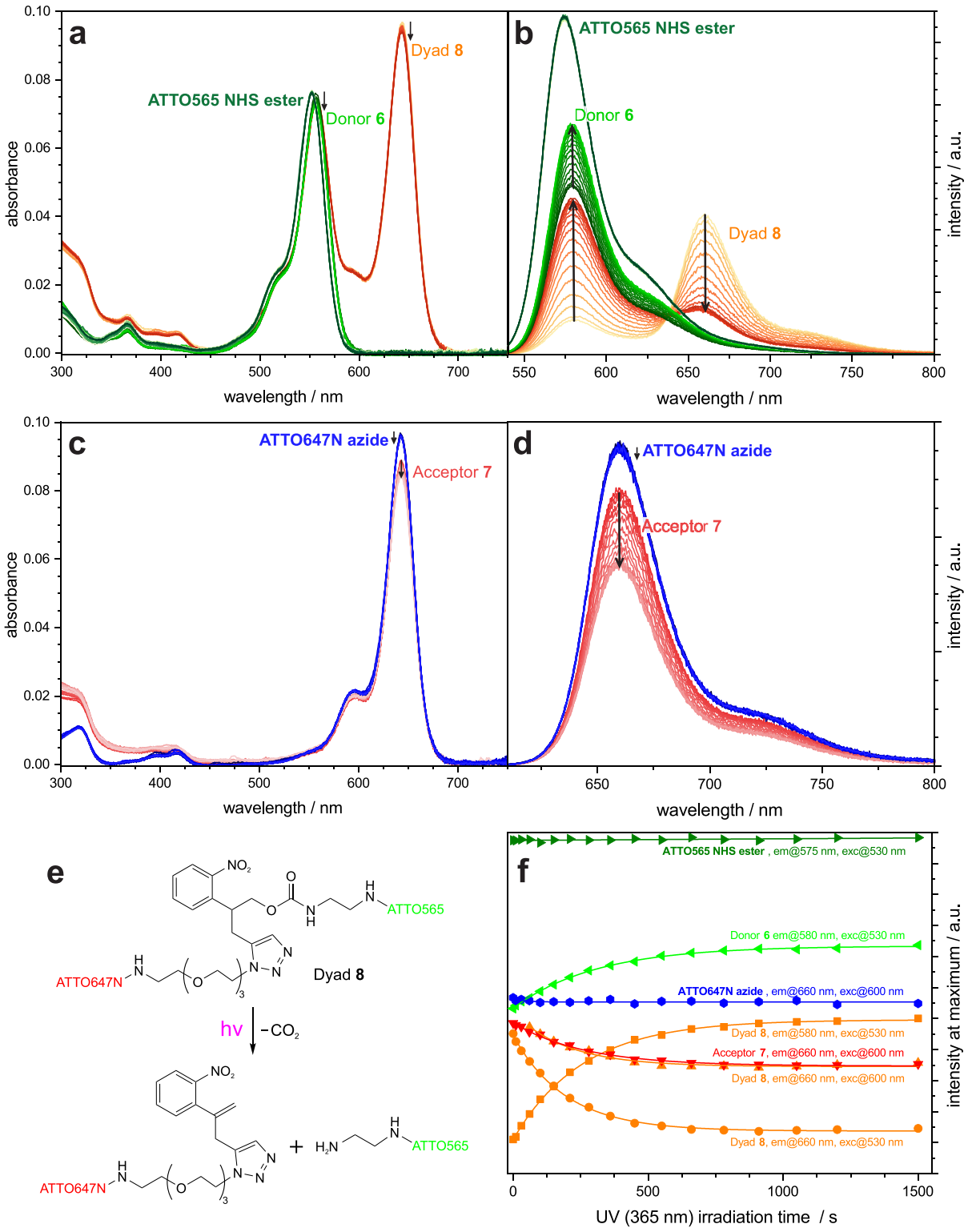

Figure 2. Spectral changes during selected irradiation times with a 365 nm LED @450 W m^{-2}. Changes of (a) absorption and (b) emission spectra of the dyad **8** (light orange → red), the reference donor **6** (dark green → green), and **ATTO565NHS ester** (light olive → dark olive) in methanol, respectively. Emissions were measured at an excitation wavelength of 530 nm. Changes of (c) absorption and (d) emission spectra of the reference acceptor **7** (red → pale red), and **ATTO647N azide** (dark blue → blue) in methanol, respectively. Emissions were measured at an excitation wavelength of 600 nm. For a better overview, the spectra of dyad **8** at 600 nm excitation are omitted here (see S.I., Figure S3). (e) The proposed main pathway of the photocleavage reaction of dyad **8**. (f) Temporal evolution of fluorescence intensities at the different wavelengths of (local) maxima for the compounds shown in (a)−(d). The data of the omitted dyad **8** spectra at 600 nm excitation are included.

and acceptor emission cannot be perfectly separated spectrally, i.e. some of the photons reaching the detector stem from the ATTO647N moiety in dyad **8**. In the spectral emission window of the acceptor in dyad **8**, between 655 and 715 nm, a

https://doi.org/10.1021/cbmi.4c00084
Chem. Biomed. Imaging 2025, 3, 199−207

single lifetime is obtained, regardless of whether the ATTO565 moiety is excited at 527 nm or the ATTO647N moiety is excited directly at 635 nm (3.67 and 3.76 ns, respectively). The lifetimes can be considered equal within the error of the measurement. Small deviations can be again explained by imperfect spectral separation.

Irradiation Experiments

We investigated the influence of 365 nm UV irradiation on all compounds characterized above. All absorption and emission spectra measured at different irradiation times are shown in Figure 2. Absorption of an UV photon can cleave the photolabile linker. The quantum efficiency of this cleavage reaction typically amounts to approximately 40% and the mechanism has been investigated in previous work.[43−46] An overview of the detailed mechanism applied to dyad **8** can also be found in the Supporting Information (Figure S1). The photoreaction splits the carbamate moiety, resulting in the release of carbon dioxide, the formation of a primary amine and an *o*-nitrostyrene compound. In the case of our dyad, the *o*-nitrostyrene product contains the acceptor dye ATTO647N whereas the primary amine is attached to the donor dye ATTO565. The proposed photocleavage reaction is shown in Figure 2e, the reference acceptor and donor react correspondingly. Additionally, a potential alternative photoreaction pathway has been identified, which results in the formation of an uncleaved nitroso compound. The subsequent cleavage of this alternative product by intramolecular rearrangement is dependent on the solvent.[46] In the case of methanol, the cleavage reaction of the nitroso product is known to occur.[46]

Under the illumination conditions used (1500 s of irradiation with a 365 nm LED at 450 $W\,m^{-2}$), the dyes ATTO565 and ATTO647N do not show significant photoreactions and only very minor photodegradation. Their absorption and fluorescence spectra remain almost constant. Likewise, fluorescence lifetimes and quantum yields remain constant within the error of measurement. In contrast, several changes are observed for the reference donor **6** under the same conditions. The absorption decreases still only marginally, but the fluorescence intensity increases significantly. This is presumably caused by the physical separation of the dye moiety from the quenching nitrophenyl moiety. After photocleavage, the system switches from potent intramolecular quenching to less efficient intermolecular quenching. The increase in intensity can be described accurately with a single exponential function ($I(t) = I_0 + \Delta I \cdot \left(1 - \exp\left(-\frac{t}{\tau}\right)\right)$ with τ = 312 s) suggesting first order kinetics for the photoreaction. The derived quantum efficiency of the cleavage reaction corresponds well to the literature value (compare S.I. Tables S1 and S2).[43] The observed enhancement in intensity can be quantified by the increase of the fluorescence quantum yield Φ from 61% to 83%. Concomitantly, the fluorescence decay kinetics change from a biexponential decay with two similar comparatively short lifetime components (2.95 ns, 73% and 2.19 ns, 27%) to a biexponential decay with one long lifetime component (4.03 ns, 75%) and one very short lifetime component (1.56 ns, 25%). The long lifetime component matches well the fluorescence lifetime of irradiated ATTO565. The cause of the short lifetime is currently not absolutely clear to us. We propose that a fraction of molecules undergoes the alternative photoreaction pathway resulting to some extent in an uncleaved nitroso-compound. In this context, we could show in Stern−Volmer experiments that nitroso-arenes exhibit significantly more efficient quenching of both used dyes than comparable nitro-arenes (for structures of nitroso cleavage products and Stern−Volmer plots with different quenchers, see the Supporting Information, Figures S1, S13 and S17, see also Figures S36−S41 and Table S6 for an extended analysis on the behavior of nitroso-arenes).

The ATTO647N fluorophore in reference acceptor **7** is less photostable than ATTO647N azide without the nitrophenyl moiety. A small decrease in absorption is found during UV irradiation as obvious from Figure 2c. Due to the decrease in absorption, we expected also a similar relative decrease in emission. However, it was found that the fluorescence intensity decreases significantly faster, i.e. the photocleavage reaction must open an additional quenching pathway. The (first order) kinetics of this additional process match the one of the photocleavage reaction. This phenomenon is also quantified by the decrease of the fluorescence quantum yield of the acceptor from 66% before irradiation to 58% after irradiation. Likewise, the fluorescence decay kinetics change from a monoexponential decay with a lifetime of 4.20 ns to a biexponential decay with fluorescence lifetimes of 4.17 and 1.3 ns with corresponding amplitudes of 89% and 11%, respectively. In the case of acceptor **7**, the quenching moiety remains attached to the dye moiety regardless of the photoreaction pathway (compare S.I., Figure S1). We assume that the longer lifetime component corresponds to the fraction of molecules undergoing the cleavage reaction to a nitrostyrene compound as shown in Figure 2e. We ascribe the shorter lifetime component to the nitroso compounds formed by the alternative photocleavage pathway, as discussed above for the donor **6**. Our hypothesis is supported by Stern−Volmer experiments. In contrast to nitro-arenes, we could show that nitroso-arenes quench the fluorescence of ATTO647N more efficiently than the fluorescence of ATTO565. Hence, the even shorter second lifetime component of acceptor **7** compared to donor **6** can be rationalized. Furthermore, we discovered that the quenching efficiency of nitrostyrene compounds is slightly higher than of comparable nitrophenyl compounds. Overall the quenching efficiency of both compound classes is comparably similar and considerably lower than that of nitroso-arenes. It seems likely that the higher quenching efficiency of nitrostyrene compounds in bimolecular quenching is not effectively reflected in the intramolecular case. In this context, it is possible that the terminal double bond of the nitrostyrene cleavage product restricts the adoptable conformations compared to the uncleaved nitrophenyl compound.

Surprisingly, the fluorescence intensity of acceptor **7** begins to increase once more following an approximate irradiation time of 1000 s. To investigate this behavior in closer detail, we irradiated the acceptor after 1500 s of 450 $W\,m^{-2}$ UV irradiation for an additional 2200 s at approximately tripled power density (for spectra, see the Supporting Information, Figure S2). During this additional irradiation time, the fluorescence quantum yield of the ATTO647N fluorophore increases again from 58% to 66%. The fluorescence lifetimes also quantify the observed changes in the emission spectra. The longer lifetime component remains constant within the accuracy of the measurement (4.17 ns (89%) versus 4.21 ns (95%)). At the same time, the shorter lifetime component increases from 1.3 ns (11%) to 1.7 ns (5%). It is known that nitroso compounds can easily dimerize in solution.[47] Additionally, they undergo a reversible photoreaction under UV

https://doi.org/10.1021/cbmi.4c00084
Chem. Biomed. Imaging 2025, 3, 199−207

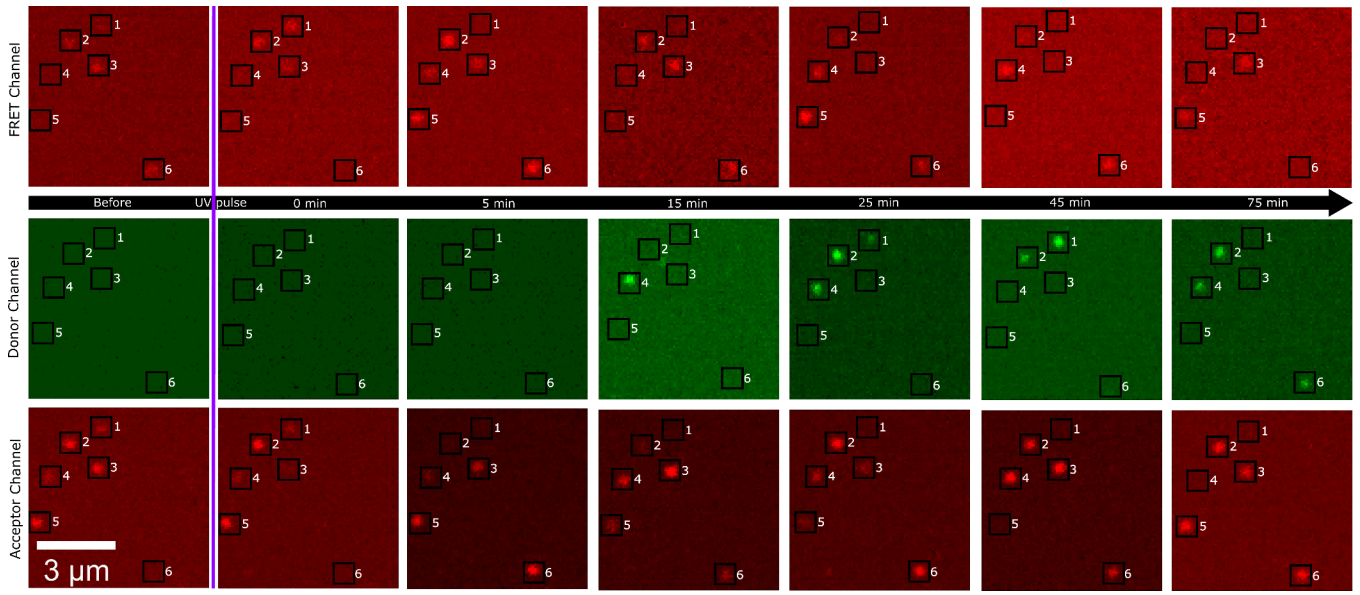

Figure 3. Series of false-color images taken from a widefield microscopy movie of dyad **8** in a tempered PVAc film before and at different times after 4 s of UV irradiation (378 nm at 50 W cm^{-2}). A selection of images recorded with 200 ms integration time is shown which were taken at the times indicated in the central time arrow. In the top row, the long wavelength channel (>655 nm) at 561 nm excitation is shown (FRET channel). In the middle row, the short wavelength channel (570−633 nm) at 561 nm excitation is displayed (donor channel). In the bottom row, the long wavelength channel at 640 nm excitation is shown (acceptor channel). All images were colored according to the respective detection channel. The vertical purple line symbolizes the UV irradiation. The imaging pixel size was 65 nm.

irradiation.[48] Both processes could cause a reduction in quenching efficiency. Lastly, we performed Fluorescence Correlation Spectroscopy (FCS) measurements of ATTO647N, the acceptor and the dyad before and after irradiation. Before irradiation, all three compounds differ in their diffusion rates according to their molecular weight. After irradiation, both dyad **8** and acceptor **7** yield the same diffusion coefficient which approaches the diffusion coefficient of ATTO647N. The latter remains unaffected by the irradiation. This result confirms that acceptor **7** and dyad **8** undergo essentially the same reaction pathway. Interestingly, we observe the appearance of a second time component with an approximately 3-fold lower diffusion coefficient compared to acceptor **7** after additional irradiation times (see Figure S18 and Table S5 in the S.I.). We currently hypothesize that under UV irradiation the nitrostyrene photocleavage product might partially oligo- or polymerize in a radical photopolymerization.

The dyad **8** displays features and behavior as basically already discussed further above for the reference donor **6** and the reference acceptor **7**. Additionally, the temporal decrease of the FRET efficiency due to the photocleavage of the covalent linker between them can be followed here. As presented in Figure 2b, at donor excitation, the originally high fluorescence intensity of the ATTO647N acceptor with a maximum at 660 nm decreases during UV irradiation while the fluorescence of the ATTO565 donor at 580 nm increases. The time constants of the exponential behavior of the first order photocleavage reaction are 258 s for the donor emission and 195 s for the acceptor emission maximum. These values, within the accuracy of their determination, are reasonably comparable. After approximately 800 s of irradiation, no noteworthy energy transfer remains. The emission spectrum can be regarded as the sum of the emission spectra of reference donor and reference acceptor (see also Figure 1b). The acceptor emission is solely caused by its direct excitation with 530 nm.

Analogous to the donor, two lifetimes $\tau_{dyad,1}$(1500 s, 527 nm) = 4.12 ns (91%) and $\tau_{dyad,2}$(1500 s, 527 nm) = 1.68 ns (9%) are found for the dyad **8** at 527 nm excitation after photocleavage when analyzing the donor fluorescence (545−620 nm). The values are reasonably similar to the lifetimes of the cleaved donor **6**. Likewise, two lifetime components $\tau_{dyad,1}$(1500 s, 527 nm) = 3.93 ns (71%) and $\tau_{dyad,2}$(1500 s, 527 nm) = 1.01 ns (29%) are observed for the dyad **8** when analyzing the acceptor fluorescence (655−715 nm) at 527 nm excitation. Again, the values are reasonably similar to the lifetimes of the cleaved acceptor **7**. At 635 nm excitation, two lifetimes $\tau_{dyad,1}$(1500 s, 635 nm) = 4.17 ns (82%) and $\tau_{dyad,2}$(1500 s, 635 nm) = 1.04 ns (18%) are obtained. The values match the lifetime components of the cleaved acceptor **7** and the above-discussed lifetimes at 527 nm excitation. Thus, it is verified that the dyad cleavage products are a mixture of the fluorescent donor and acceptor cleavage products.

Microscopic Evaluation

We tested the performance of our novel photocleavable dyad in single molecule microscopy measurements by embedding picomolar amounts of dyad **8** in thin polymer films. As polymer test system, we selected polyvinyl acetate (PVAc, Sigma-Aldrich, M_W = 184000 g mol^{-1}), since it is soluble in methanol and its glass transition temperature is just above ambient temperature.[49] Hence, in measurements at room temperature we expected sufficiently low mobility and small translational diffusion coefficients which cannot be reliably determined with classical single molecule tracking (SMT). Our method requires the spectral separation of fluorescence into two distinct wavelength channels for ATTO565 and for ATTO647N emission, respectively. We checked for crosstalk between the short wavelength channel (570−633 nm, henceforth called the donor channel) and the long wavelength channel (>655 nm, henceforth called the FRET channel when using 561 nm excitation and acceptor channel when using 640

https://doi.org/10.1021/cbmi.4c00084
Chem. Biomed. Imaging 2025, 3, 199−207

nm excitation, see also the Supporting Information, section S1.6). For this purpose, we separately embedded trace amounts of donor **6** and acceptor **7** in thin PVAc films and conducted a regular measurement, i.e. we used alternating laser excitation[50] with a 561 and 640 nm laser. The cleavage of the NPPOC linker was achieved with a 378 nm UV-laser. All lasers were combined and coupled into a widefield illumination setup. No leakage of donor fluorescence into the FRET channel or of acceptor fluorescence into the donor channel was observed. Likewise, no direct excitation of the acceptor fluorescence with 561 nm excitation or of donor fluorescence with 640 nm could be detected (see the Supporting Information, Figures S27−S29). Given the recorded bulk spectra in Figure 1, it seems likely that under the chosen measurement conditions both donor leakage and direct acceptor excitation exist, but they are significantly below the detectable noise threshold. No significant influence of UV irradiation (378 nm laser @ 50 W cm^{-2} for up to 5 s) on the polymer film or the photometric properties of either donor or acceptor was observed. In this context, it is noteworthy that on the single molecule level a few random bright signals can be observed in the donor channel with 561 nm excitation even in blank tests using thin PVAc films without any dye additives. We assume these signals to stem from various impurities in the polymer, e.g. remaining catalyst from the synthesis. However, the impurities are spatially sparse enough to be distinguished from dye signals. Since no leakage into the FRET channel or excitation at 640 nm was observed, they do not impede our method. In Figure 3, a representative sequence of single molecule microscopy images is shown. We can demonstrate that the signals in the FRET channel take dozens of minutes to become weaker and eventually disappear while corresponding signals start appearing in the donor channel (compare first and second row of Figure 3). Intensity-time traces of the six identified FRET pairs in Figure 3 can be found in the Supporting Information (Figure S30). The continued emission from most ATTO647N moieties in the acceptor channel (third row in Figure 3) proves that in almost all cases the interrupted FRET is not due to photobleaching of the acceptor, but caused by energy donor and energy acceptor diffusing beyond the efficient FRET range, i.e. distances larger than the determined Förster distance. Thereby, the general suitability of the novel dyad **8** for our FEDUP method is verified.

The image sequence shows further noteworthy effects. As usual for single molecule time traces, all fluorescence signals (donor, acceptor and FRET) exhibit notable blinking behavior. Consequently, the disappearance of a FRET signal in a single frame does not necessarily result in the immediate appearance of a corresponding donor signal and vice versa. Nevertheless, the blinking kinetics do not impede the determination of a reliable diffusion coefficient, as the final evaluation relies on the sum of the intensities of several donor−acceptor pairs to ascertain sufficient statistics. The blinking behavior also influences the control measurement with 640 nm excitation. Hence, a positive control signal in every frame of the acceptor channel is not feasible. However, the last frame in which a signal appears in the acceptor channel can be assumed to be the point in time when photobleaching of the acceptor occurred. Typically, a good correlation between photobleaching and the appearance of donor signals can be observed. All together, we performed proof-of-principle experiments to show that we have a powerful method to evaluate very low diffusion coefficients in polar systems by observing the temporal evolution of the energy transfer between a donor and an acceptor after photocleavage. The possibility to do this on a single molecule (pair) level allows us also to address heterogeneities in diffusion on the long time scales required for highly viscous systems.

CONCLUSION AND OUTLOOK

We successfully synthesized a novel photocleavable fluorescent dye dyad for the purpose of diffusion measurements below the limit of accurate measurements with single molecule tracking. Initially, the dyad exhibits an energy transfer efficiency of about 80% in methanol. After photocleavage, energy donor and energy acceptor diffuse away from each other independently causing a gradual loss in energy transfer efficiency. In contrast to our previous approach,[1] the dyad reported here meets two additional demands: it can be dissolved in polar media and the two orthogonal labeling sites of the linker can be efficiently cleaved with UV-A irradiation. We fully characterized the system in regard to its spectral properties, with particular attention paid to any changes introduced by photocleavage. We analyzed the evolution of the fluorescence behavior after photocleavage of the dyad with bulk experiments and on the single molecule level. Apart from fluorescence intensities, we also investigated the corresponding fluorescence lifetime changes which could be used equivalently. Finally, we demonstrated the suitability of the dyad for single molecule diffusion imaging with a proof-of-concept measurement in a thin PVAc film. The time-intensity traces of single donor−acceptor pairs are subject to significant fluctuations uncorrelated to the distance dependency of the energy transfer. However, the data still allows for a statistical analysis of the diffusional behavior. After this general evaluation of the novel dyad, we will continue with a detailed investigation of diffusion in highly viscous systems. This is, however, beyond the scope of the current paper and will be represented at a later stage.

ASSOCIATED CONTENT

Supporting Information

The Supporting Information is available free of charge at https://pubs.acs.org/doi/10.1021/cbmi.4c00084.

Equipment, measurement protocols, syntheses instructions, NMR spectra, MS spectra, a complete scheme of the photocleavage mechanism, excluded absorption and fluorescence spectra, quantum yield measurements, Stern−Volmer experiments, FCS curves, TCSPC curves, excluded microscopy images, microscopic time-intensity traces, and a HPLC chromatogram of dyad **8** (PDF)

AUTHOR INFORMATION

Corresponding Author

Dominik Wöll − *Institute of Physical Chemistry, RWTH Aachen University, 52074 Aachen, Germany;* orcid.org/0000-0001-5700-4182; Phone: +49 (0)241 8098624; Email: woell@pc.rwth-aachen.de

Author

Damian Schöngen − *Institute of Physical Chemistry, RWTH Aachen University, 52074 Aachen, Germany;* orcid.org/0009-0007-9515-1053

Complete contact information is available at: https://pubs.acs.org/10.1021/cbmi.4c00084

https://doi.org/10.1021/cbmi.4c00084
Chem. Biomed. Imaging 2025, 3, 199−207

Notes

The authors declare no competing financial interest.

■ ACKNOWLEDGMENTS

The authors thank Hridya M. Biju for her assistance in the microscopy measurements, Thomas Schmidt for providing most of the codes for the analysis of the single molecule videos, Kristofer Weinberg for his help with large parts of the synthesis and quenching experiments, and Leon Trottenberg for general discussions. We thank Cornelia Vermeeren for her assistance with the HPLC experiments. We thank ATTO-TEC GmbH for discussion on the fluorophores. We thank the German Research Foundation for partially funding this project within the Collaborative Research Center SFB 985.

■ REFERENCES

(1) Dill, M.; Baier, M. C.; Mecking, S.; Wöll, D. Enhanced Accuracy of Single-Molecule Diffusion Measurements with a Photocleavable Energy-Transfer Dyad. *Angew. Chem., Int. Ed.* **2013**, *52*, 12435−12438.
(2) Jacobs, M. H. In *Diffusion Processes*; Jacobs, M. H., Ed.; Springer: 1935; pp 1−145.
(3) Pellin, M.; Stair, P.; Xiong, G.; Elam, J.; Birrell, J.; Curtiss, L.; George, S.; Han, C.; Iton, L.; Kung, H.; Kung, M.; Wang, H.-H. Mesoporous Catalytic Membranes: Synthetic Control of Pore Size and Wall Composition. *Catal. Lett.* **2005**, *102*, 127−130.
(4) Tsushima, S.; Teranishi, K.; Hirai, S. Water Diffusion Measurement in Fuel-Cell SPE Membrane by NMR. *Energy J.* **2005**, *30*, 235−245.
(5) Schacher, F.; Ulbricht, M.; Müller, A. H. E. Self-Supporting, Double Stimuli-Responsive Porous Membranes From Polystyrene-block-poly(N,N-dimethylaminoethyl Methacrylate) Diblock Copolymers. *Adv. Funct. Mater.* **2009**, *19*, 1040−1045.
(6) Nunnery, G.; Hershkovits, E.; Tannenbaum, A.; Tannenbaum, R. Adsorption of Poly(Methyl Methacrylate) on Concave Al2O3 Surfaces in Nanoporous Membranes. *Langmuir* **2009**, *25*, 9157−9163.
(7) Fradin, C. On the Importance of Protein Diffusion in Biological Systems: The Example of the Bicoid Morphogen Gradient. *BBA-Proteins Proteom* **2017**, *1865*, 1676−1686.
(8) Guo, L.; Har, J. Y.; Sankaran, J.; Hong, Y.; Kannan, B.; Wohland, T. Molecular Diffusion Measurement in Lipid Bilayers over Wide Concentration Ranges: A Comparative Study. *ChemPhysChem* **2008**, *9*, 721−728.
(9) Pincet, F.; Adrien, V.; Yang, R.; Delacotte, J.; Rothman, J. E.; Urbach, W.; Tareste, D. FRAP to Characterize Molecular Diffusion and Interaction in Various Membrane Environments. *PLoS One* **2016**, *11*, No. e0158457.
(10) Sezgin, E.; Schneider, F.; Galiani, S.; Urbančič, I.; Waithe, D.; Lagerholm, B. C.; Eggeling, C. Measuring Nanoscale Diffusion Dynamics in Cellular Membranes with Super-Resolution STED−FCS. *Nat. Protoc* **2019**, *14*, 1054−1083.
(11) Thomas, D. L.; Lythgoe, M. F.; Pell, G. S.; Calamante, F.; Ordidge, R. J. The Measurement of Diffusion and Perfusion in Biological Systems Using Magnetic Resonance Imaging. *Phys. Med. Biol.* **2000**, *45*, R97.
(12) Wachsmuth, M. Molecular Diffusion and Binding Analyzed with FRAP. *Protoplasma* **2014**, *251*, 373−382.
(13) Bosch, P. J.; Kanger, J. S.; Subramaniam, V. Classification of Dynamical Diffusion States in Single Molecule Tracking Microscopy. *Biophys. J.* **2014**, *107*, 588−598.
(14) Wolff, J. O.; Scheiderer, L.; Engelhardt, T.; Engelhardt, J.; Matthias, J.; Hell, S. W. MINFLUX Dissects the Unimpeded Walking of Kinesin-1. *Science* **2023**, *379*, 1004−1010.
(15) Saxton, M. J.; Jacobson, K. Single-Particle Tracking: Applications to Membrane Dynamics. *Annu. Rev. Bioph. Biom.* **1997**, *26*, 373−399.
(16) Zawodzinski, T.; Neeman, M.; Sillerud, L. O.; Gottesfeld, S. Determination of Water Diffusion Coefficients in Perfluorosulfonate Ionomeric Membranes. *J. Phys. Chem.* **1991**, *95*, 6040−6044.
(17) Westrin, B. A.; Axelsson, A.; Zacchi, G. Diffusion Measurement in Gels. *J. Controlled Release* **1994**, *30*, 189−199.
(18) Rharbi, Y.; Yekta, A.; Winnik, M. A. A Method for Measuring Oxygen Diffusion and Oxygen Permeation in Polymer Films Based on Fluorescence Quenching. *Anal. Chem.* **1999**, *71*, 5045−5053.
(19) Stempfle, B.; Dill, M. J.; Winterhalder, M.; Müllen, K.; Wöll, D. Single Molecule Diffusion and Its Heterogeneity during the Bulk Radical Polymerization of Styrene and Methyl Methacrylate. *Polym. Chem.* **2012**, *3*, 2456−2463.
(20) Maris, J. J. E.; Fu, D.; Meirer, F.; Weckhuysen, B. M. Single-Molecule Observation of Diffusion and Catalysis in Nanoporous Solids. *Adsorption* **2021**, *27*, 423−452.
(21) Iwao, R.; Yamaguchi, H.; Niimi, T.; Matsuda, Y. Single-Molecule Tracking Measurement of PDMS Layer during Curing Process. *Physica A* **2021**, *565*, 125576.
(22) Bi, W.; Yeow, E. K. L. Single-Particle Tracking of the Formation of a Pseudoequilibrium State Prior to Charged Microgel Cluster Formation at Interfaces. *NPG Asia Mater.* **2020**, *12*, 1−11.
(23) Pagès, G.; Gilard, V.; Martino, R.; Malet-Martino, M. Pulsed-Field Gradient Nuclear Magnetic Resonance Measurements (PFG NMR) for Diffusion Ordered Spectroscopy (DOSY) Mapping. *Analyst* **2017**, *142*, 3771−3796.
(24) Kärger, J.; Freude, D.; Haase, J. Diffusion in Nanoporous Materials: Novel Insights by Combining MAS and PFG NMR. *Processes* **2018**, *6*, 147.
(25) Sprague, B. L.; McNally, J. G. FRAP Analysis of Binding: Proper and Fitting. *Trends Cell Biol.* **2005**, *15*, 84−91.
(26) Ishikawa-Ankerhold, H. C.; Ankerhold, R.; Drummen, G. P. C. Advanced Fluorescence Microscopy Techniques—FRAP, FLIP, FLAP, FRET and FLIM. *Molecules* **2012**, *17*, 4047−4132.
(27) Wöll, D. Fluorescence Correlation Spectroscopy in Polymer Science. *RSC Adv.* **2013**, *4*, 2447−2465.
(28) Gupta, A.; Sankaran, J.; Wohland, T. Fluorescence Correlation Spectroscopy: The Technique and Its Applications in Soft Matter. *Physical Sciences Reviews* **2019**, *4*, 20170104.
(29) Shen, H.; Tauzin, L. J.; Baiyasi, R.; Wang, W.; Moringo, N.; Shuang, B.; Landes, C. F. Single Particle Tracking: From Theory to Biophysical Applications. *Chem. Rev.* **2017**, *117*, 7331−7376.
(30) Wöll, D.; Braeken, E.; Deres, A.; De Schryver, F.; Uji-i, H.; Hofkens, J. Polymers and single molecule fluorescence spectroscopy, what can we learn? *Chemi. Soc. Rev.* **2009**, *38*, 313−328.
(31) Mortensen, K. I.; Churchman, L. S.; Spudich, J. A.; Flyvbjerg, H. Optimized Localization Analysis for Single-Molecule Tracking and Super-Resolution Microscopy. *Nat. Methods* **2010**, *7*, 377−381.
(32) Michalet, X.; Berglund, A. J. Optimal Diffusion Coefficient Estimation in Single-Particle Tracking. *Phys. Rev. E* **2012**, *85*, 061916.
(33) Enderlein, J.; Toprak, E.; Selvin, P. R. Polarization Effect on Position Accuracy of Fluorophore Localization. *Opt. Express, OE* **2006**, *14*, 8111−8120.
(34) Balzarotti, F.; Eilers, Y.; Gwosch, K. C.; Gynnå, A. H.; Westphal, V.; Stefani, F. D.; Elf, J.; Hell, S. W. Nanometer Resolution Imaging and Tracking of Fluorescent Molecules with Minimal Photon Fluxes. *Science* **2017**, *355*, 606−612.
(35) Weinstain, R.; Slanina, T.; Kand, D.; Klán, P. Visible-to-NIR-Light Activated Release: From Small Molecules to Nanomaterials. *Chem. Rev.* **2020**, *120*, 13135−13272.
(36) Fückel, B.; Köhn, A.; Harding, M. E.; Diezemann, G.; Hinze, G.; Basché, T.; Gauss, J. Theoretical investigation of electronic excitation energy transfer in bichromophoric assemblies. *J. Chem. Phys.* **2008**, *128*, 074505.
(37) Hasan, A.; Stengele, K.-P.; Giegrich, H.; Cornwell, P.; Isham, K. R.; Sachleben, R. A.; Pfleiderer, W.; Foote, R. S. Photolabile Protecting Groups for Nucleosides: Synthesis and Photodeprotection Rates. *Tetrahedron* **1997**, *53*, 4247−4264.
(38) Giegrich, H.; Eisele-Bühler, S.; Hermann, C.; Kvasyuk, E.; Charubala, R.; Pfleiderer, W. New Photolabile Protecting Groups in

https://doi.org/10.1021/cbmi.4c00084
Chem. Biomed. Imaging 2025, 3, 199−207

Nucleoside and Nucleotide Chemistry—Synthesis, Cleavage Mechanisms and Applications. *Nucleos Nucleot* **1998**, *17*, 1987−1996.
(39) Yi, H.; Maisonneuve, S.; Xie, J. Synthesis, Glycosylation and Photolysis of Photolabile 2-(2-Nitrophenyl)Propyloxycarbonyl (NPPOC) Protected Glycopyranosides. *Org. Biomol. Chem.* **2009**, *7*, 3847−3854.
(40) Mutai, K. Intramolecular Fluorescence Quenching Effect by P-Nitrophenyl and p-Nitrophenoxy Groups. *bull. Chem. Soc. Jpn.* **1971**, *44*, 2537−2541.
(41) Pandith, A.; Kumar, A.; Kim, H. S. Imidazole-appended 9,10-anthracenedicarboxamide probe for sensing nitrophenols and selective determination of 2,4,6-trinitrophenol in an EtOH−water medium. *RSC Adv.* **2016**, *6*, 68627−68637.
(42) www.atto-tec.com/?cPath=37_45&cat=c45_R-0--Werte--FRET--r-0-werte-fret.html.
(43) Walbert, S.; Pfleiderer, W.; Steiner, U. E. Photolabile Protecting Groups for Nucleosides: Mechanistic Studies of the 2-(2-Nitrophenyl)Ethyl Group. *Helv. Chim. Acta* **2001**, *84*, 1601−1611.
(44) Wöll, D.; Smirnova, J.; Pfleiderer, W.; Steiner, U. E. Highly Efficient Photolabile Protecting Groups with Intramolecular Energy Transfer. *Angew. Chem., Int. Ed.* **2006**, *45*, 2975−2978.
(45) Wöll, D.; Laimgruber, S.; Galetskaya, M.; Smirnova, J.; Pfleiderer, W.; Heinz, B.; Gilch, P.; Steiner, U. E. On the Mechanism of Intramolecular Sensitization of Photocleavage of the 2-(2-Nitrophenyl)Propoxycarbonyl (NPPOC) Protecting Group. *J. Am. Chem. Soc.* **2007**, *129*, 12148−12158.
(46) Wöll, D.; Smirnova, J.; Galetskaya, M.; Prykota, T.; Bühler, J.; Stengele, K.-P.; Pfleiderer, W.; Steiner, U. E. Intramolecular Sensitization of Photocleavage of the Photolabile 2-(2-Nitrophenyl)-Propoxycarbonyl (NPPOC) Protecting Group: Photoproducts and Photokinetics of the Release of Nucleosides. *Chem. Eur. J.* **2008**, *14*, 6490−6497.
(47) Beaudoin, D.; Wuest, J. D. Dimerization of Aromatic C-Nitroso Compounds. *Chem. Rev.* **2016**, *116*, 258−286.
(48) Hadjoudis, E.; Tsoka, A.; Wettermark, G. A Flash Photolytic Study of O-Nitrosotoluene. *J. Photochem.* **1978**, *8*, 233−238.
(49) Adhikari, A. N.; Capurso, N. A.; Bingemann, D. Heterogeneous Dynamics and Dynamic Heterogeneities at the Glass Transition Probed with Single Molecule Spectroscopy. *J. Chem. Phys.* **2007**, *127*, 114508.
(50) Kapanidis, A. N.; Laurence, T. A.; Lee, N. K.; Margeat, E.; Kong, X.; Weiss, S. Alternating-Laser Excitation of Single Molecules. *Acc. Chem. Res.* **2005**, *38*, 523−533.

https://doi.org/10.1021/cbmi.4c00084
Chem. Biomed. Imaging 2025, 3, 199−207